Biogeosciences

Constraints on the applicability of the organic temperature proxies $U_{37}^{K'}$, TEX$_{86}$ and LDI in the subpolar region around Iceland

M. Rodrigo-Gámiz[1,a], **S. W. Rampen**[1], **H. de Haas**[2], **M. Baas**[1], **S. Schouten**[1], and **J. S. Sinninghe Damsté**[1]

[1]NIOZ Royal Netherlands Institute for Sea Research, Department of Marine Organic Biogeochemistry, P.O. Box 59, 1790 AB Den Burg, Texel, the Netherlands
[2]NIOZ Royal Netherlands Institute for Sea Research, Marine Research Facilities, Den Burg, Texel, the Netherlands
[a]present address: Instituto Andaluz de Ciencias de la Tierra (IACT), CSIC-Universidad de Granada, Granada, Spain

Correspondence to: M. Rodrigo-Gámiz (martarodrigo@ugr.es)

Abstract. Subpolar regions are key areas for studying natural climate variability due to their high sensitivity to rapid environmental changes, particularly through sea surface temperature (SST) variations. Here, we have tested three independent organic temperature proxies ($U_{37}^{K'}$; TEX$_{86}$; and the long-chain diol index, LDI) regarding their potential applicability for SST reconstruction in the subpolar region around Iceland. $U_{37}^{K'}$, TEX$_{86}$ and TEX$_{86}^L$ temperature estimates from suspended particulate matter showed a substantial discrepancy with instrumental data, while long-chain alkyl diols were below the detection limit at most of the stations. In the northern Iceland Basin, sedimenting particles revealed a seasonality in lipid fluxes, i.e., high fluxes of alkenones and glycerol dialkyl glycerol tetraethers (GDGTs) were measured during late spring and during summer and high fluxes of long-chain alkyl diols during late summer. The flux-weighted average temperature estimates had a significant negative (ca. 2.3 °C for $U_{37}^{K'}$) and positive (up to 5 °C for TEX$_{86}$) offset with satellite-derived SSTs and temperature estimates derived from the underlying surface sediment. $U_{37}^{K'}$ temperature estimates from surface sediments around Iceland correlate well with summer mean sea surface temperatures, while TEX$_{86}$-derived temperatures correspond with both annual and winter mean 0–200 m temperatures, suggesting a subsurface temperature signal. Anomalous LDI-SST values in surface sediments and low mass flux of 1,13- and 1,15-diols compared to 1,14-diols suggest that *Proboscia* diatoms are the major sources of long-chain alkyl diols in this area rather than eustigmatophyte algae, and therefore the LDI cannot be applied in this region.

1 Introduction

Several organic proxies, based on different lipids, have been developed for estimating sea surface temperatures (SSTs) (Brassell et al., 1986; Schouten et al., 2002; Rampen et al., 2012). One of the first organic temperature proxies developed was the $U_{37}^{K'}$ index (Prahl and Wakeham, 1987), which is based on the relative abundances of C_{37} di- and tri-unsaturated long-chain ketones. Culture and core top studies demonstrated that haptophyte algae adjust the degree of alkenone unsaturation in response to their growth temperature, and the $U_{37}^{K'}$ index is strongly related to average annual mean SST (Prahl and Wakeham, 1987; Müller et al., 1998). However, the $U_{37}^{K'}$ index may be affected by variations in nutrient concentrations, light limitation, and diagenesis (e.g., Hoefs et al., 1998; Gong and Hollander, 1999; Prahl et al., 2003; Rontani et al., 2013).

Another organic temperature proxy commonly used in the last decade is the TEX$_{86}$ (Schouten et al., 2002, 2013), based on a ratio of glycerol dialkyl glycerol tetraethers (GDGTs) with a varying number of cyclopentane moieties in the membrane lipids of marine Thaumarchaeota (Sinninghe Damsté et al., 2002). The TEX$_{86}$ is strongly correlated with satellite-derived annual mean SST in global core top data sets (Kim et al., 2008, 2010; Ho et al., 2014). However, marine Thaumarchaeota occur throughout the whole water column (e.g., Karner et al., 2001), and thus the TEX$_{86}$ often reflects the water temperature of subsurface water masses (e.g., Huguet et al., 2007). The TEX$_{86}$-SST calibrations by Kim et al. (2010) distinguish between low-temperature (< 15 °C, TEX$_{86}^L$) and

high-temperature ($> 15\,°C$, TEX_{86}^{H}) regions, which takes into account an increased relative abundance of the crenarchaeol regioisomer in subtropical regions. Furthermore, a subsequent recalibration of TEX_{86}^{L} with depth-integrated annual mean temperatures from 0 to 200 m water depth was established following evidence of abundant subsurface Thaumarchaeota in Antarctic regions (Kim et al., 2012b). The TEX_{86} seems to be less affected by diagenesis than the $U_{37}^{K'}$ index (Schouten et al., 2004; Kim et al., 2009b), but it can be biased by contributions of soil-derived isoprenoid GDGTs in coastal marine sediments, which can be assessed by the BIT (Branched and Isoprenoid Tetraether) index (Hopmans et al., 2004). A terrestrial effect on TEX_{86} may be substantial when BIT values are > 0.3 (Weijers et al., 2006, 2009), although it has been noted that this threshold depends on the location (cf. Schouten et al., 2013). More clues may be obtained by correlating the BIT index with TEX_{86} values, where a significant correlation could indicate the impact of terrestrial input.

Recently, Rampen et al. (2012) proposed the long-chain diol index (LDI), based on the fractional abundances of C_{30} 1,15-alkyl diol relative to those of C_{28} 1,13-, C_{30} 1,13- and C_{30} 1,15-alkyl diols (hereafter referred to as diols), showing a strong correlation with annual mean SST in globally distributed surface sediments. The LDI proxy seems to be independent of salinity but the effect of degradation or nutrient limitation is not yet known. C_{28} and C_{30} 1,13-diols and C_{30} and C_{32} 1,15-diols have been reported in eustigmatophyte algae (Volkman et al., 1992, 1999; Gelin et al., 1997; Méjanelle et al., 2003), but since these algae are not widely reported from open-ocean settings and the diol distributions in cultured eustigmatophytes differ from those found in the natural environment, there are still uncertainties about the biological source of long-chain 1,13- and 1,15-diols in marine sediments (Versteegh et al., 1997, 2000; Rampen et al., 2012). Besides 1,13- and 1,15-diols, 1,14-diols have also been identified in marine sediments. These lipids have been reported in *Proboscia* diatoms, which are thought to be their source (Sinninghe Damsté et al., 2003; Rampen et al., 2007), although they have also been identified in the marine alga *Apedinella radians* (Rampen et al., 2011).

SST reconstructions derived from the various organic molecular proxies can differ as proxies may reflect temperatures of different seasons or different habitat depths, and proxies may also be affected by environmental factors other than temperature. Importantly, the use of organic proxies in high-latitude regions is often problematic. Previous studies have raised doubts about the applicability of alkenone paleothermometry at high latitudes, due to the nonlinearity of the relationship of $U_{37}^{K'}$ index with SST at low temperatures ($< 6\,°C$) and the high, erratic abundance of the $C_{37:4}$ alkenone (e.g., Sikes and Volkman, 1993; Rosell-Melé et al., 1994; Rosell-Melé, 1998; Rosell-Melé and Comes, 1999; Conte et al., 2006). Concerning the TEX_{86}, studies in subpolar regions have observed significant deviations in reconstructed SST, even with the TEX_{86}^{L} calibration (Ho et al.,

2014, and references therein), as well as a substantial scatter in the correlation (Kim et al., 2010). The LDI has been applied thus far in the midlatitudes of the Northern (Rampen et al., 2012; Lopes dos Santos et al., 2013; Rodrigo-Gámiz et al., 2014) and Southern Hemispheres (Smith et al., 2013) but not in high-latitude regions, although surface sediments from high latitudes were included in the surface sediment calibration (cf. Rampen et al., 2012).

To test and constrain the application of the different organic temperature proxies at high latitudes, we have collected suspended particulate matter, sedimenting particles, and marine surface sediments from several stations distributed around Iceland. This region is of particular interest for climate studies because it is in the transition zone between polar and temperate climate regimes and is thereby subjected to large variations in hydrographic conditions (Ólafsson, 1999). Thus, this high-latitude region presents an ideal setting for testing and applying organic temperature proxies, including the novel LDI, in cold regions.

2 Material and methods

2.1 Oceanographic setting

The oceanographic configuration around Iceland is predominantly characterized by the interplay of two water masses, i.e., warm and saltier Atlantic water versus cold Arctic or subpolar waters. From the south flows the Irminger Current (IC) – a branch of the warm and salty Atlantic current, which moves northwards along the west Iceland coast and continues along the north Iceland coast, extending down to several hundred meters (Hopkins, 1991) (Fig. 1). Flowing southward from north to west Iceland, the East Greenland Current (EGC) transports cold and low-salinity polar waters. A branch of the EGC, the East Iceland Current (EIC), turns eastward and flows southward along the east coast of Iceland (Hopkins, 1991). The EGC carries icebergs and sea ice formed in the Arctic Ocean and in East Greenland fjords (Sigtryggsson, 1972). The wide transitional zone between the polar waters and the Atlantic waters in the Denmark Strait is defined as the polar front. The position of this front is known to vary on annual, interannual and longer timescales (Malmberg and Jónsson 1997; Sigtryggsson, 1972). During episodes of extensive sea ice, the contribution of polar waters from the EGC to EIC is relatively large and responsible for carrying sea ice, icebergs and cold, low-salinity waters to the northwest coast of Iceland (Sigtryggsson, 1972).

The polar front is also expressed in the phytoplankton blooms around Iceland. In the Arctic or subpolar waters, the early onset of stratification in spring gives rise to a rapid shallowing of the mixed layer and triggers the early spring bloom (in early April) north of Iceland. In the south of Iceland, the weakly stratified water column in the Atlantic water and an associated deep mixed layer delays the spring bloom
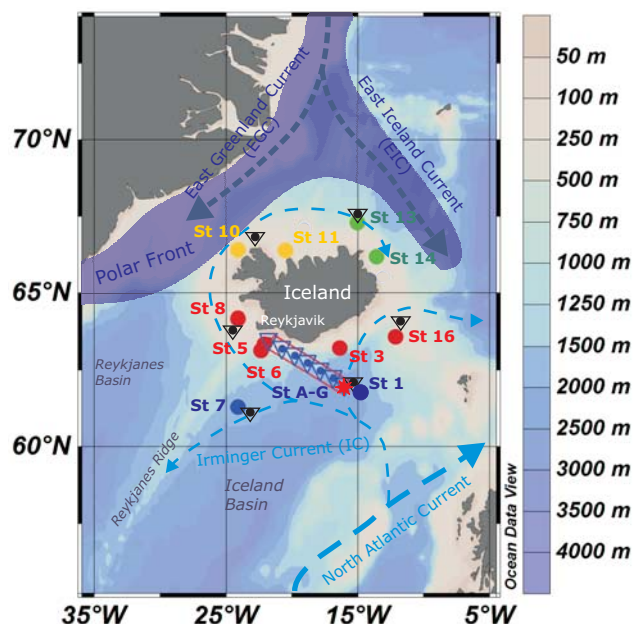
Figure 1. Bathymetric map of the study area with the location of the different sampling stations around Iceland. Filled circles indicate surface sediment stations with color coding according to the area of location, i.e., yellow and green for the northern stations, red for the shallow stations in the south of Iceland and blue for the deep southern stations. Black and blue inverse triangles with filled circles indicate surface particulate matter stations around Iceland sampled during July 2011 and the transect from Iceland Basin (St A) to Reykjavik (St G) sampled during July 2012, respectively. The red star indicates the location of sediment trap deployment. Dashed blue arrows show the theoretical circulation of the different water masses.

(e.g., Zhai et al., 2012, and references therein). The spring bloom initiation varies by up to a month between different regions around Iceland. Within the southern Iceland shelf region, the spring bloom generally starts in near-shore waters (mid-May) and is delayed with increasing distance from the coast, where it is affected by the interaction between runoff and wind regime (Thordardottir, 1986).

2.2 Sample collection

Sample material was collected around Iceland during long-chain diol cruises (Cruise Report 64PE341, de Haas, 2011; and Cruise Report 64PE357, Baas and Koning, 2012) in the summer of 2011 and 2012 on board the R/V *Pelagia* (Fig. 1, Table 1). During July 2011, suspended particulate matter (SPM) from a water depth of ca. 5 m and surface sediments were collected at different stations (St) around Iceland (Table 1), and a sediment trap was deployed at 1850 m water depth at St 1 (water depth at this station is 2255 m), located in the northern part of the Iceland Basin, to recover sinking particulate matter (Fig. 1). During July 2012, SPM was collected at 20 and 50 m water depth in a transect from the site of

the sediment trap deployment to Reykjavik (Fig. 1, Table 1) after the sediment trap was recovered.

SPM was obtained by filtering through 142 mm diameter glass-fiber filters (GFFs) with a pore diameter of 0.7 μm using a McLane Research Laboratories WTS 6-1-142LV in situ pump installed on a CTD (conductivity–temperature–depth) rosette frame. The CTD measured the vertical distribution of temperature, salinity, turbidity, oxygen and fluorescence. SPM filters were frozen directly after filtration and stored at $-20\,°C$ until analysis.

A McLane Parflux 78H-21 sediment trap (aperture area: $0.5\,\text{m}^2$) was set to collect sinking material every 17.5 days in a 21-cup automated sampling carousel covering one complete annual cycle (Table 2). Prior to mooring the sediment trap, the sample cups were filled with a mercuric-chloride-poisoned and borax-buffered solution of seawater collected from the deployment depth ($1\,\text{g}\,\text{L}^{-1}$ of $HgCl_2$; pH ~ 8.5). After recovery of the sediment trap, collecting cups were stored in the dark at $4\,°C$.

Sediment cores were taken using a multicorer, sliced into 1 cm wide sections and frozen onboard. The upper 1 cm was analyzed for biomarkers.

2.3 Extraction and lipid fractionation

In the laboratory, any larger "swimmers" were removed from the sediment trap collecting cups prior to subdividing into two volumetrically split aliquots using a Folsom wet splitter (Sell and Evans, 1982) with a precision of $> 95\,\%$. One half was stored in the dark at $4\,°C$, and the second half was used for lipid analysis. The trap material was centrifuged at 3000 rpm for 15 min, followed by pipetting the water layer and washing with bidistilled H_2O ($3\times$) to remove the $HgCl_2$ and borax solution. The sediment trap samples ($n = 21$) and surface sediment samples ($n = 10$) were freeze-dried, homogenized in agate mortar and extracted after the addition of extracted diatomaceous earth in an accelerated solvent extractor 350 (ASE 350, DIONEX) using a solvent mixture of $9 : 1$ ($v : v$) dichloromethane (DCM) to methanol (MeOH) at $100\,°C$ and 7.6×10^6 Pa. The solvent from all the extracts was reduced by TurboVap LV Caliper, dried over Na_2SO_4 and concentrated under a stream of N_2, yielding a total lipid extract (TLE). Three internal standards were added to the TLE from the sediment trap samples, i.e., 10-nonadecanone (C_{19} ketone) for alkenones, C_{22} 7,16-diol for long-chain diols and the C_{46} glycerol trialkyl glycerol tetraether (GTGT) for GDGTs (Huguet et al., 2006). Activated copper and DCM were added to the TLEs of the sediment trap samples that were found to contain elemental sulfur. After being stirring overnight with a small stirring bar, the TLEs were filtered over a pipette column containing Na_2SO_4 and dried under a stream of N_2.

SPM filters ($n = 14$) were freeze-dried and half of each filter was saponified according to de Leeuw et al. (1983) by refluxing for 1 h with 1 M KOH in MeOH (96 %). Af-

Table 1. Location, depth and other information on each material collected at different stations around Iceland.

Station	Latitude	Longitude	Depth (m.b.s.l.)	Core length (cm)	Volume pumped (L)
Sediment trap					
1	N 61°59.757′	W 16°00.191′	1850		
SPM collected around Iceland July 2011					
1	N 62°0.008′	W 16°0.016′	5		no data
7	N 61°29.917′	W 24°10.333′	5		26
8	N 64°17.583′	W 24°8.811′	5		25
10	N 66°40.647′	W 24°10.794′	5		130
13	N 67°30.098′	W 15°4.109′	5		164
16	N 63°59.132′	W 12°12.472′	6		10
SPM collected along transect July 2012					
A	N 61°59.757′	W 16°00.191′	20		36
A	N 61°59.757′	W 16°00.191′	50		229
B	N 62°14.963′	W 16°51.877′	50		199
C	N 62°29.635′	W 17°50.287′	50		183
D	N 62°44.568′	W 18°48.771′	50		216
E	N 62°58.981′	W 19°47.270′	50		220
F	N 63°12.696′	W 20°44.820′	50		219
G	N 63°27.319′	W 21°44.951′	50		219
Sediment cores					
1	N 62°0.019′	W 15°59.951′	2255	18	
3	N 63°21.972′	W 16°37.696′	240	5	
5	N 63°34.996′	W 22°8.624′	188	15	
6	N 63°14.294′	W 22°33.685′	315	15	
7	N 61°29.913′	W 24°10.335′	1628	28	
8	N 64°17.591′	W 24°8.825′	260	33	
10	N 66°40.647′	W 24°10.770′	241	30	
11	N 66°37.999′	W 20°50.006′	367	10	
13	N 67°30.098′	W 15°4.153′	884	10	
14	N 66°18.186′	W 13°58.369′	262	no data	

ter cooling, the solvent was acidified with 2 N HCl in MeOH ($1:1$, $v:v$) to a pH of 2, and transferred to a separatory funnel containing bidistilled H_2O. The residual filters were further extracted using $H_2O:MeOH$ ($1:1$, $v:v$, ×1), MeOH (×1) and DCM (×3), and all solvents were combined in the separatory funnel. The DCM layer in the separatory funnel was separated from the $H_2O:MeOH$ layer and the remaining $H_2O:MeOH$ layer was extracted three times with DCM. DCM layers were combined and rotary evaporated to near dryness. Thereafter, the obtained extracts were acid hydrolyzed (3 h reflux with 2 N HCl:MeOH, $1:1$, $v:v$) and neutralized with 1 M KOH in MeOH (96 %). Then 3 mL bidistilled H_2O was added to the acid hydrolyzed extracts and the lipids were extracted using DCM (4×). The filter material remaining after base hydrolysis was also acid hydrolyzed (3 h reflux with 2 N HCl:MeOH, $1:1$, $v:v$). After cooling, the solvent was neutralized with 1 M KOH in MeOH (96 %) and transferred to a separatory funnel containing bidistilled H_2O. Subsequently, the acid-hydrolyzed

residual filters were extracted using $H_2O:MeOH$ ($1:1$, $v:v$, ×1), MeOH (×1) and DCM (×3), and the extracts were combined in the separatory funnel. The DCM layer was collected and the remaining $H_2O:MeOH$ layer was extracted three times with DCM. All extracts, obtained by saponification and acid hydrolysis, were combined, dried under N_2, eluted in DCM over a pipette column containing Na_2SO_4 and dried under a stream of N_2.

Extracts of SPM, descending particles and surface sediments were separated into apolar, ketone (containing alkenones) and polar fractions (containing GDGTs and long-chain diols) by column chromatography using a Pasteur pipette filled with Al_2O_3 (activated for 2 h at 150 °C) using $9:1$ ($v:v$) hexane:DCM, $1:1$ ($v:v$) hexane:DCM, and $1:1$ ($v:v$) DCM:MeOH as the eluents, respectively.

Table 2. Sampling intervals in the sediment trap and fluxes of lipids. For proxy values and derived temperatures, see Table S2.

Period	Start (mm/dd/yy)	Sampling interval (days)	Bulk flux (mg m^{-2} day^{-1})	C$_{37:2}$+ C$_{37:3}$ flux (µg m^{-2} day^{-1})	GDGT-0 flux (µg m^{-2} day^{-1})	TEX$_{86}$-GDGTs[1] flux (µg m^{-2} day^{-1})	Crenarchaeol flux (µg m^{-2} day^{-1})	Sat. 1,14-diols flux (ng m^{-2} day^{-1})	Unsat. 1,14-diols flux (ng m^{-2} day^{-1})	LDI-diol[2] flux (ng m^{-2} day^{-1})
1	07/15/11	16.5	166	115	2800	640	2600	500	280	160
2	08/01/11	17.5	9.3	0.91	220	53	174	32	n.d.	10.7
3	08/19/11	17.5	21	0.32	280	55	240	13.6	2.8	4.8
4	09/05/11	17.5	75	1.03	3000	550	2900	550	3700	120
5	09/23/11	17.5	188	n.d.	2600	610	2600	770	1620	147
6	10/10/11	17.5	49	1.04	1960	380	1800	450	530	96
7	10/27/11	17.5	7.5	0.10	370	94	330	23	2.0	6.3
8	11/14/11	17.5	28	0.11	440	132	390	33	52	7.4
9	12/01/11	17.5	28	0.32	1170	380	1130	86	154	29
10	12/19/11	17.5	16.8	0.27	600	220	590	31	49	11.0
11	01/05/12	17.5	16.6	0.18	720	270	720	57	85	16.2
12	01/23/12	17.5	11.2	0.20	760	300	740	46	n.d.	12.0
13	02/09/12	17.5	11.2	0.21	900	340	890	41	59	19.2
14	02/26/12	17.5	9.3	0.12	410	159	390	33	45	9.0
15	03/15/12	17.5	18.3	0.02	280	83	198	41	20	3.5
16	04/01/12	17.5	7.5	0.08	390	156	370	6.8	3.4	2.3
17	04/19/12	17.5	3.7	0.04	173	64	163	3.8	5.1	1.50
18	05/06/12	17.5	108	54	4900	690	4000	540	420	165
19	05/24/12	17.5	160	134	14 400	2300	11 000	410	470	155
20	06/10/12	17.5	134	74	10 900	1970	9700	185	260	106
21	06/27/12	17.5	45	2.6	1870	380	1550	33	32	9.8

n.d.: not detected; [1] GDGTs with one, two and three cyclopentane moieties and the crenarchaeol regioisomer; [2] C$_{28}$ and C$_{30}$ 1,13- and C$_{30}$ 1,15-diol.

2.3.1 Alkenone analysis

The ketone fractions were dried under N$_2$ and redissolved in an appropriate volume (20–100 µL) of hexane. Analysis of the di- (C$_{37:2}$) and tri-unsaturated (C$_{37:3}$) alkenones was performed on an Hewlett Packard 6890 gas chromatograph (GC) using a 50 m CP Sil-5 column (0.32 mm diameter, film thickness of 0.12 µm), equipped with a flame ionization detector and helium as the carrier gas. The temperature of the oven was initially 70 °C and increased, with a rate of 20 °C per minute to 200 °C and subsequently with a rate of 3 °C per minute to 320 °C, at which it was held for 25 min. Alkenone relative abundances were determined by the integration of relevant peak areas.

The U$_{37}^{K'}$ index (Eq. 1) was used to estimate SSTs according to the equation by Prahl and Wakeham (1987):

$$U_{37}^{K'} = [C_{37:2}]/([C_{37:2}] + [C_{37:3}]). \tag{1}$$

U$_{37}^{K'}$ values were converted to SSTs using the global core top calibration of Müller et al. (1998):

$$U_{37}^{K'} = 0.033 \times SST + 0.044. \tag{2}$$

The calibration error associated with the U$_{37}^{K'}$ is 1.5 °C (Müller et al., 1998). Five samples were run in duplicate, resulting in a standard deviation (SD) of 0.02 or better, equivalent to 0.8 °C.

2.3.2 GDGT analysis

Polar fractions of the extracts, containing the GDGTs, were dried under a stream of N$_2$, redissolved by sonication (5 min) in 200 µL hexane : propanol (99 : 1, v : v), and filtered through 0.45 µm polytetrafluoroethylene (PTFE) filters. GDGTs were analyzed by high-performance liquid chromatography–mass spectrometry (HPLC/MS) following the method described by Schouten et al. (2007). Samples were analyzed on an Agilent 1100 series LC/MSD SL. A Prevail Cyano column (150 mm × 2.1 mm, 3 mm) was used with hexane : isopropanol (99 : 1, v : v) as an eluent. After the first 5 min, the eluent increased by a linear gradient up to 1.8 % isopropanol (vol) over the next 45 min at a flow rate of 0.2 mL min^{-1}. Scanning was performed in single-ion monitoring (SIM) mode. The identification and quantification of the GDGT isomers and C$_{46}$ GTGT standard was achieved by integrating the peak areas of relevant peaks in m/z 1302, 1300, 1298, 1296, 1292, 1050, 1036, 1022 and 744 mass chromatograms.

The TEX$_{86}$ and TEX$_{86}^{L}$ index were calculated following Kim et al. (2010):

$$TEX_{86} = ([GDGT2] + [GDGT3] + [cren']/([GDGT1]$$
$$+ [GDGT2] + [GDGT3] + [cren']) \tag{3}$$
$$TEX_{86}^{L} = ([GDGT2]/([GDGT\ 1]$$
$$+ [GDGT2] + [GDGT3]), \tag{4}$$

where numbers correspond to isoprenoid GDGTs from marine Thaumarchaeota with 1, 2 or 3 cyclopentane moieties, and cren$'$ corresponds to crenarchaeol regioisomer, which has the antiparallel configuration to crenarchaeol (Sinninghe Damsté et al., 2002).

TEX_{86} and TEX_{86}^{L} values were converted to SSTs using calibrations (Eqs. 5, 6) proposed by Kim et al. (2010):

$$\text{SST} = 81.5 \times \text{TEX}_{86} - 26.6 \tag{5}$$

$$\text{SST} = 67.5 \times \log(\text{TEX}_{86}^{L}) + 46.9. \tag{6}$$

Calibration errors are 5.2 and 4 °C, due to the large scatter in the polar regions (Kim et al., 2010).

Furthermore, the Kim et al. (2012b) TEX_{86}^{L} temperature calibration with 0–200 m water depth was also used:

$$T(0 - 200\,\text{m}) = 50.8 \times \log(\text{TEX}_{86}^{L}) + 36.1. \tag{7}$$

The BIT index, a measure for soil versus marine organic matter input in marine sediments, was calculated according to Hopmans et al. (2004):

$$\begin{aligned}
\text{BIT} = &([\text{GDGT-I}] + [\text{GDGT-II}] + [\text{GDGT-III}])/ \\
&([\text{crenarchaeol}] + [\text{GDGT-I}] \\
&+ [\text{GDGT-II}] + [\text{GDGT-III}]),
\end{aligned} \tag{8}$$

where roman numerals correspond to the major branched GDGTs (see Hopmans et al., 2004).

A total of 17 samples were run in duplicate for TEX_{86} and the BIT, showing an SD of 0.09, equivalent to 1.0 °C or better for TEX_{86}^{L}, and an SD of 0.002 or better for the BIT index.

2.3.3 Long-chain diol analysis

After GDGT analysis, polar fractions were silylated by the addition of 15 µL N,O-bis(trimethylsilyl)trifluoroacetamide (BSTFA) and pyridine and heating in an oven at 60 °C for 20 min. Long-chain diol distributions were analyzed using a Thermo trace gas chromatograph (GC) Ultra coupled to Thermo DSQ MS. A 25 m CP Sil-5 fused silica capillary column was used (25 m × 0.32 mm; film thickness = 0.12 µm) with helium as the carrier gas. The column was directly inserted into the electron impact ion source of the DSQ quadrupole MS with an ionization energy of 70 eV. Samples were dissolved in 50–100 µL ethyl acetate and injected at 70 °C. The oven was programmed to increase first at a rate of 20 °C per minute to 130 °C and then at a rate of 4 °C per minute to the final temperature of 320 °C (held for 25 min). Various long-chain diols and the C_{22} 7,16-diol standard were quantified using an SIM of m/z 299, 313, 327, 341, and 187, respectively (cf. Rampen et al., 2012). The selected ions contributed on average 6.5 % to the total ion counts for unsaturated long-chain diols, 9.7 % to the total ion counts for the saturated long-chain diols, and 19 % to the total ion counts for the C_{22} 7,16-diol standard.

The Long-chain Diol Index (LDI) was calculated and converted to SST following Rampen et al. (2012):

$$\begin{aligned}
\text{LDI} = &[C_{30}1, 15\text{-diol}]/([C_{28}1, 13\text{-diol}] + [C_{30}1, 13\text{-diol}] \\
&+ [C_{30}1, 15\text{-diol}])
\end{aligned} \tag{9}$$

$$\text{LDI} = 0.033 \times \text{SST} + 0.095 \tag{10}$$

The calibration error for the LDI is 2.0 °C (Rampen et al., 2012). Replicate analysis of three samples showed a mean SD of 0.023, equivalent to 0.7 °C.

3 Results

3.1 Suspended particulate matter

SPM was collected during two cruises: in July 2011 at six stations around Iceland at ca. 5 m water depth, and in July 2012 in a transect (St A–G) from the northern Iceland Basin to Reykjavik at 50 m and, at some locations, also at 20 m water depth (Fig. 1).

Alkenones were detected in all samples except from St 13. Values for the $U_{37}^{K'}$ index varied between 0.26 and 0.53 (or 6.4 and 14.7 °C when translated into temperature) in the SPM around Iceland during summer 2011 (Fig. 2a, open green diamonds) and between 0.26 and 0.45 (corresponding to 6.5 to 12.5 °C) during summer 2012 (Fig. 2b, open green diamonds). GDGTs were detected in all samples and the TEX_{86} values ranged between 0.49 and 0.55 (corresponding to 13.1 to 17.9 °C) in SPM around Iceland (Fig. 2a, dark blue circles) and between 0.34 and 0.50 (corresponding to 1.0 to 14.4 °C) along the transect of 2012 (Fig. 2b, dark blue circles). TEX_{86}^{L} varied between 0.28 and 0.32 (corresponding to 9.4 to 13.7 °C) around Iceland (Fig. 2a, open blue circles) and between 0.22 and 0.29 (corresponding to 2.5 to 10.6 °C) along the transect (Fig. 2b, open blue circles). Long-chain alkyl diols were not detected in SPM around Iceland collected during summer 2011 (Fig. 2a), while C_{28} and C_{30} 1,13- and 1,14-diols and C_{30} and C_{32} 1,15-diols were only detected in SPM collected at St A, B, F and G during the transect in the summer of 2012. LDI values varied between 0.08 and 0.49, corresponding to −0.4 to 12 °C when converted into temperature (Fig. 2b, open brown squares). Values for $U_{37}^{K'}$, TEX_{86} and LDI and corresponding temperatures are reported in Supplement Table S1.

3.2 Descending particulate matter

Sinking particulate matter was collected between 15 July 2011 and 16 July 2012 at St 1, using a sediment trap deployed at 1850 m water depth. Bulk sediment fluxes varied between 4 and 165 mg m^{-2} day^{-1} (Fig. 3b), with high fluxes occurring in July, September and October 2011 and from May to July 2012. C_{37} alkenone fluxes varied between 0.02 and 130 µg m^{-2} day^{-1}, peaking during spring and summer, i.e., in July 2011 and in May and
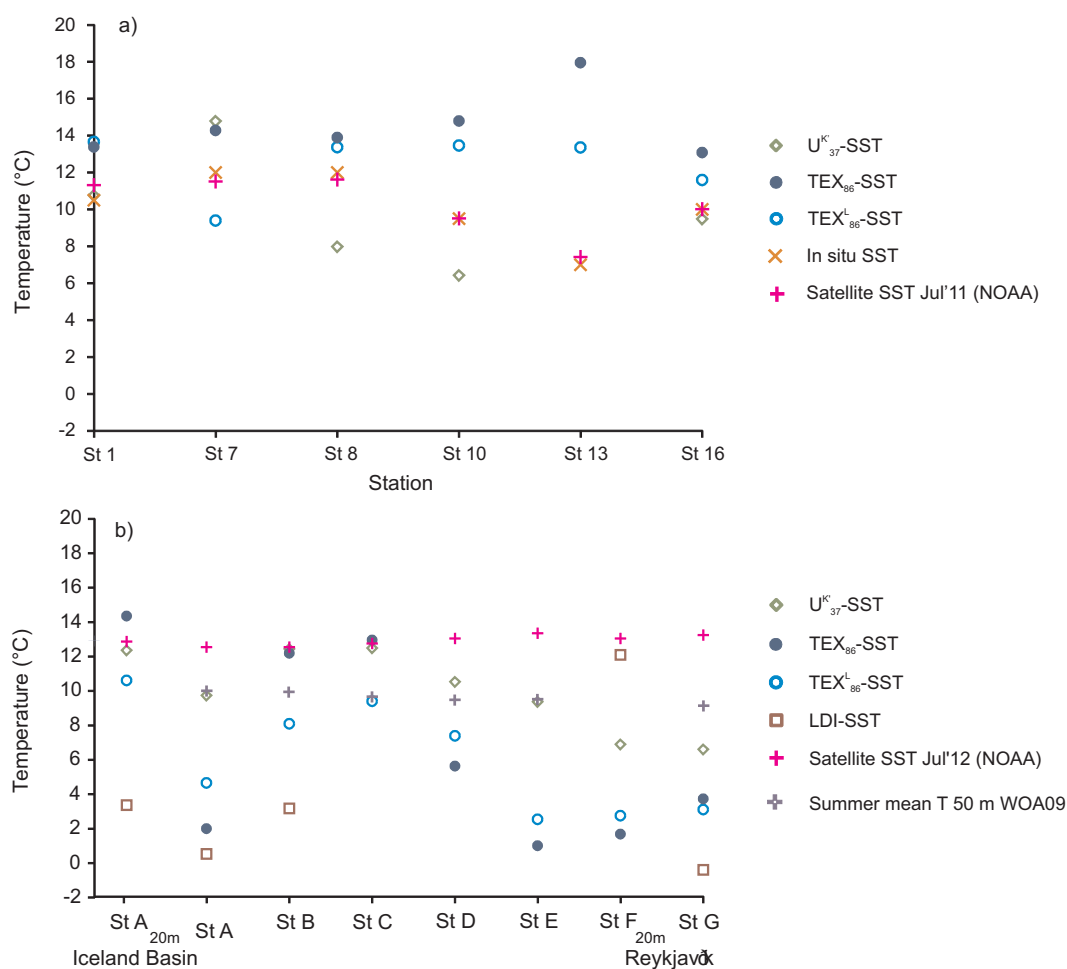
Figure 2. $U_{37}^{K'}$-, TEX_{86}^{L}- and LDI-derived temperatures from SPM obtained at the different sampling stations around Iceland. Panel **(a)**: SPM collected at ca. 5 m water depth during July 2011; panel **(b)**: SPM collected at 50 m water depth collected during July 2012. Open green diamonds indicate $U_{37}^{K'}$-derived temperatures; filled dark blue circles indicate TEX_{86}-derived temperatures using calibration by Kim et al. (2010a); open blue circles indicate TEX_{86}^{L}-derived temperatures using calibration by Kim et al. (2010a); open brown squares indicate LDI-derived temperatures. Orange symbols indicate in situ SST measured with the CTD; pink symbols indicate satellite SST from NOAA remote-sensing records at the time of sample collection, i.e., July 2011 and July 2012, and purple symbols indicate summer mean temperatures at 50 m water depth from the WOA09 (World Ocean Atlas) database.

June 2012 (Table 2; Fig. 3c). Fluxes of the GDGTs used for the calculation of the TEX_{86} index ranged between 53 and 2300 µg m^{-2} day^{-1} with highest values recorded from May to June 2012 (Table 2; Fig. 3d). GDGT-0 and crenarchaeol fluxes followed the same pattern as those of the GDGTs used in the TEX_{86}, ranging from minimum values of ca. 170 µg m^{-2} day^{-1} to a maximum of 15 and 11 mg m^{-2} day^{-1}, respectively (Fig. 3d). Values for the BIT index were always below < 0.01. Fluxes of long-chain 1,13- and 1,15-diols used in the LDI were low compared to alkenones and GDGT fluxes and varied between 1.5 and 170 ng m^{-2} day^{-1}, with highest values recorded during July, September and October 2011 and from May to June 2012 (Table 2; Fig. 3e). Generally, the flux of the C_{30} 1,15-diol was always low (up to 2 ng m^{-2} day^{-1}) or even below

the detection limit for most of the intervals. The fluxes of saturated and monounsaturated C_{28} and C_{30} 1,14-diols were substantially higher than those of the 1,13- and 1,15-diols (Fig. 3e). The highest summed mass flux of the C_{28} and C_{30} monounsaturated 1,14-diols was recorded in September 2011 with a flux of 3.7 µg m^{-2} day^{-1} (Fig. 3e). C_{28} and C_{30} saturated 1,14-diol fluxes varied between minimum values of 3.8 ng m^{-2} day^{-1} during the second half of April and maximum values of 770 ng m^{-2} day^{-1}, with high fluxes recorded during July, September and October 2011 and May and June 2012 (Table 2; Fig. 3e).

$U_{37}^{K'}$-based temperatures derived from settling particles ranged from 5.3 to 11.4 °C (Fig. 4), with maximum values recorded at the end of summer (September 2011) and late winter (end of February 2012) and minimum values in
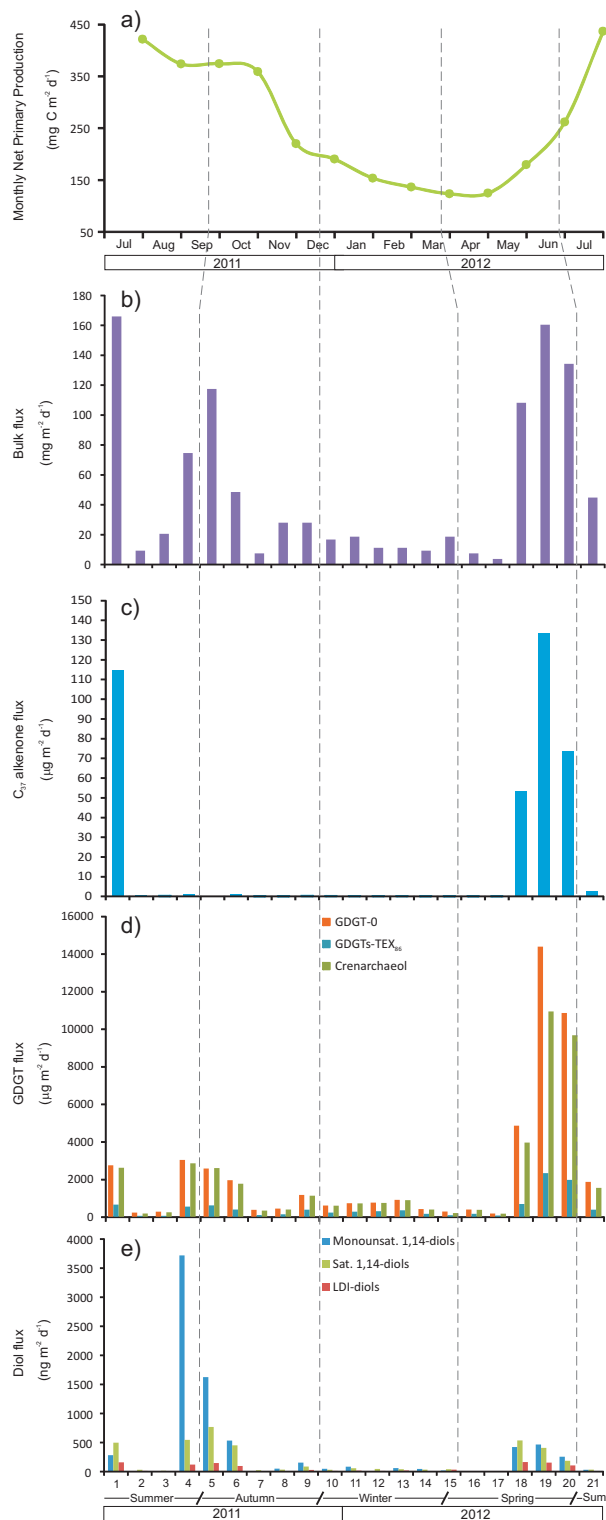
Figure 3. Panel **(a)**: variations in the net primary productivity from July 2011 to July 2012 derived from OceanColor Web (Behrenfeld and Falkowski, 1997). Bar plots of fluxes of **(b)** particulate matter, **(c)** C_{37} alkenones, **(d)** isoprenoid GDGTs, and **(e)** long-chain diols as determined from sediment trap data. Numbers refer to sampling intervals specified in Table 2.

spring (from May to June 2012) (Fig. 4, green line), when the highest flux is observed. Temperature estimates based on TEX_{86} varied between 6.8 and 9.6 °C (Fig. 4, dark blue line) and those based on TEX_{86}^L varied between 12.6 and 17.5 °C (Fig. 4, light blue line), with the highest values recorded from November 2011 to April 2012. TEX_{86}^L-temperature estimates based on the 0–200 m calibration showed absolute values ranging from 10.3 to 13.9 °C (Fig. 4, red line). For sampling periods when 1,13- and 1,15-diols were detected, the LDI-based temperatures vary between −2.7 and 0.2 °C (Fig. 4, brown line and open squares). Values for $U_{37}^{K'}$, TEX_{86} and LDI and corresponding temperatures are reported in Table S2.

3.3 Surface sediments

Surface sediments were collected in July 2011 from 10 stations around Iceland (Fig. 1; Table 1). The $U_{37}^{K'}$ index varied between 0.26 and 0.53 in the surface sediments, yielding SST estimates between 7 and 11 °C for St 13 and St 7, respectively (Fig. 5, open green diamonds). TEX_{86} ranged between 0.36 and 0.44 with SST estimates between 2.4 and 9.2 °C (Fig. 5, dark blue circles). TEX_{86}^L ranged between 0.19 and 0.33, resulting in TEX_{86}^L-derived temperatures between −1.2 °C at St 13 and 14 °C at S. 1 (Fig. 5, open light blue circles) or between −0.1 and 11.4 °C using the 0–200 m calibration (Fig. 5, open red circles). LDI values varied between 0.02 and 0.27, with SST estimates between −2.1 and 5.2 °C, reaching high values in the coastal stations, St 3 and St 8 (Fig. 5, open brown squares). Values for $U_{37}^{K'}$, TEX_{86} and LDI and corresponding temperatures are reported in Table S3.

4 Discussion

4.1 $U_{37}^{K'}$

Long-chain alkenones are produced by several haptophyte algal species thriving in the photic zone (Volkman et al., 1980, 1995; Marlowe et al., 1984) and are, therefore, thought to reflect SST. Although previous studies of cold polar waters (< 4 °C) of the North Atlantic have shown relatively high abundances of $C_{37:4}$ (e.g., Sicre et al., 2002), the C_{37} alkenones in SPM, descending particles and surface sediments around Iceland comprised only $C_{37:3}$ and $C_{37:2}$, and no $C_{37:4}$ was detected. Comparison of $U_{37}^{K'}$-derived temperatures with in situ temperatures showed generally lower $U_{37}^{K'}$-derived temperatures, differing by up to 3.4 °C for SPM around Iceland (Fig. 2a) and by up to 6.6 °C for the SPM transect (Fig. 2b). Reduced temperature differences (up to 2.6 °C) were observed when we compared $U_{37}^{K'}$-derived SSTs with summer temperatures at 50 m water depth (Fig. 2b, purple crosses; derived from the World Ocean Atlas (WOA) 09 database; Locarnini et al., 2010), at which most of the SPM was recovered from the transect. Possibly, the alkenones col-
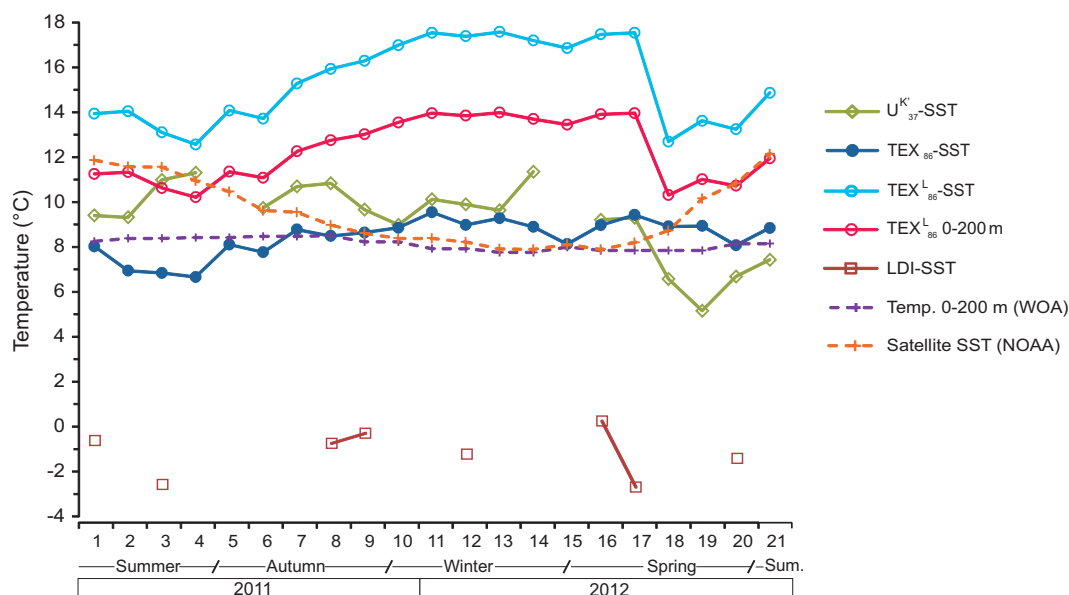
Figure 4. Changes in temperatures derived from $U_{37}^{K'}$ (green line and diamonds), TEX_{86} (dark blue line and open circles), TEX_{86}^L (light blue line and open circles), TEX_{86}^L 0–200 m (light red line and open circles), and LDI (brown line and open squares) in descending particles over one complete annual cycle, from July 2011 to July 2012. Numbers refer to sampling intervals specified in Table 2, and data points represent the center of collection intervals. Satellite temperatures (from AVHRR, NOAA) at St 1 during the sampling period are indicated with a dashed orange line and 0–200 mean temperatures from WOA09 are indicated with a dashed purple line.
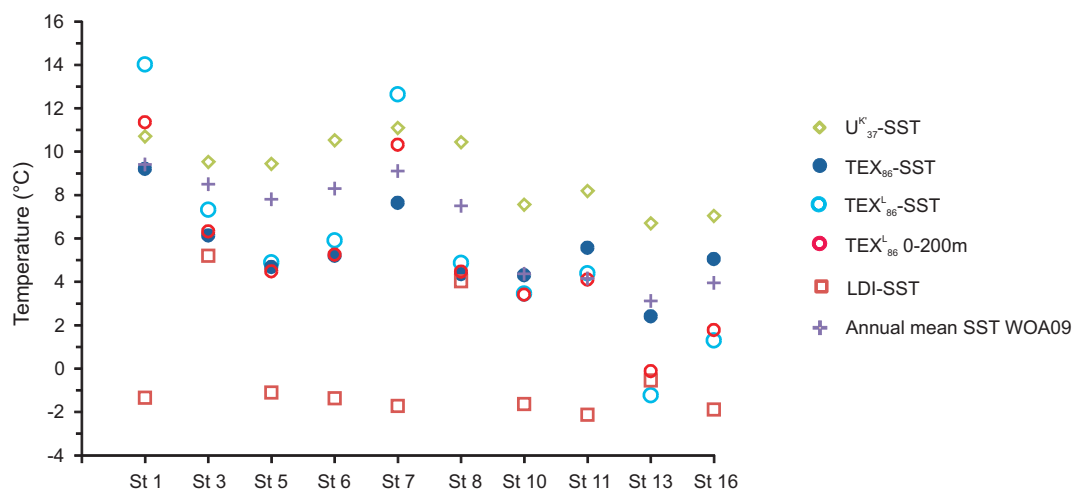

Figure 5. Temperatures in surface sediments from stations around Iceland from $U_{37}^{K'}$ (open green diamonds), TEX_{86} (dark blue circles), TEX_{86}^L (open light blue circles), TEX_{86}^L 0–200 m (open red circles) and LDI (open brown squares) derived . Annual mean SSTs at each station obtained from the WOA09 database are indicated as purple crosses.

lected in the SPM did not represent recently produced material but alkenones synthesized over several months. Since SPM was collected in July, the warmest month of the year, the $U_{37}^{K'}$ would reflect lower temperatures if the signal also reflected material synthesized in the preceding colder months.

Interestingly, $U_{37}^{K'}$-derived SSTs of sedimenting particles also show major discrepancies compared to satellite SSTs, i.e., somewhat higher $U_{37}^{K'}$-derived SSTs were observed from

January to mid-May (differing by around 2–3 °C) and lower temperatures from mid-May to July (differing by up to 4.9 °C) (Fig. 4, green line and open diamonds) at the time of the highest alkenone flux (Fig. 3c). The underestimation of temperatures by $U_{37}^{K'}$ in sedimenting particles in July is consistent with the discrepancy between $U_{37}^{K'}$-derived and in situ temperature observed for SPM for the same time period. The application of the $U_{37}^{K'}$ SPM calibration proposed by Conte et

al. (2006) also results in a general overestimation (by up to 2.7 °C) of $U^{K'}_{37}$-derived SSTs in both the SPM and sedimenting particles (data not shown), suggesting that the difference between $U^{K'}_{37}$-derived and in situ temperature is not due to calibration issues.

Higher $U^{K'}_{37}$-derived SST in cold periods could perhaps be attributed to the gradual sinking of alkenones that were produced in preceding warmer time periods. Similar discrepancies, i.e., $U^{K'}_{37}$-SSTs overestimating in situ winter temperatures and underestimating in situ summer temperatures in the surface mixed layer, have been previously described for alkenones in sediment traps from other subpolar and midlatitude regions (e.g., Sikes et al., 2005; Harada et al., 2006; Seki et al., 2007; Yamamoto et al., 2007; Lee et al., 2011). In the Mediterranean, Arabian Sea and the Pacific, $U^{K'}_{37}$-SSTs lower than in situ SST during a high alkenone flux have been attributed to either alkenone production at the thermocline depth or to nutrient deficiency (e.g., Ternois et al., 1997; Prahl et al., 2000; Harada et al., 2006; Popp et al., 2006).

A compilation of previous sediment trap studies in the North Atlantic has shown that the $U^{K'}_{37}$ export signal produced in surface waters is not equivalent to the vertically transported $U^{K'}_{37}$ signal collected in the underlying sediment traps or accumulating in surface sediments (Rosell-Melé and Prahl, 2013). In the current study, the $U^{K'}_{37}$-SST value obtained for the surface sediment at St 1, ca. 10.7 °C (Fig. 5), corresponds well with annual mean SST from WOA09 of 9.4 °C (Locarnini et al., 2010) but is higher than the $U^{K'}_{37}$-derived temperature of the flux-weighted average of our sediment trap data (7.1 °C; Table 3). This difference seems mainly due to the anomalously low $U^{K'}_{37}$-derived temperatures at the time of high alkenone fluxes. These discrepancies could result from (1) a bias from advected or resuspended alkenones by oceanic currents masking the local pattern of export production from overlying surface waters (e.g., Prahl et al., 2001), as has been previously noted in the NE Atlantic (Rosell-Melé et al., 2000); (2) an unusual subsurface production of alkenones in the summer of 2011 leading to a cold bias for that year only; or (3) selective degradation of alkenones when they are sedimenting on the sea floor (e.g., Hoefs et al., 1997; Rontani et al., 2013).

The calculation of sinking velocities for alkenones can be done following the approach of Fischer and Karakas (2009) and Mollenhauer et al. (2015) and uses the offsets between minimum and maximum temperatures recorded in the calculated $U^{K'}_{37}$ temperatures and SST. Maximum derived temperatures are obtained for sampling periods 4 (5–23 September 2011) and 14 (26 February–15 March 2012), while the maximum satellite SSTs are in the months June and July (Fig. 4 and Table S2). The minimum alkenone-derived temperature is during sampling period 19 (24 May–10 June 2012), and minimum satellite SSTs are in February–April 2012 (Fig. 4 and Table S2). Based on this, average sinking velocities (0–1850 m) for alkenones are ca. 25–30 m day^{-1}, which is substantially lower compared to the sink-

ing rates of alkenones in the filamentous upwelling region off Cape Blanc (Müller and Fischer, 2001). However, our estimates are quite uncertain as alkenone-derived temperatures do not show a clear seasonal trend compared to the seasonal SST trend (Fig. 4). Furthermore, an offset of more than 2 months between alkenone production and their fluxes recorded at 1850 m water depth seems in contrast with the similar timing of alkenone flux patterns and net primary production (derived from OceanColor Web; Behrenfeld and Falkowski, 1997) over this period (Fig. 3a, c).

In surface waters in the Norwegian–Iceland seas, the abundances of coccolithophore communities are usually higher during the high-bloom period (summer) than during the low-bloom period (late summer and fall) (Baumann et al., 2000). Furthermore, high alkenone fluxes were also previously observed from April to June, with a rapid decline until August, in 1989 in the NE Atlantic (Rosell-Melé et al., 2000). Consequently, the increased flux of alkenones in spring likely reflects the spring bloom. $U^{K'}_{37}$-derived SSTs at the peak flux of alkenones thus likely reflect spring and early summer temperatures, in agreement with previous studies from high-latitude sites (Sikes et al., 1997; Ternois et al., 1998; Rosell-Melé et al., 2000; Sicre et al., 2005, 2006; Conte et al., 2006; Hanna et al., 2006). Degradation during transport in the water column or in the oxic sediment layer is expected to result in higher $U^{K'}_{37}$-derived SSTs, since the $C_{37:3}$ has a higher degradation rate than $C_{37:2}$ (Prahl et al., 1988, 2003; Hoefs et al., 1998; Gong and Hollander, 1999), and this is indeed what we observe in the surface sediment compared to the flux-weighted mean (Table 3). An alteration of alkenones in the sea floor may thus explain the mismatch between surface sediment signal and flux-weighted mean signal. Finally, it is important to keep in mind that the data obtained with the sediment trap only provides a snapshot in time, while the surface sediment stores information collected over decades to centuries. Thus, the offset of the weighted average $U^{K'}_{37}$-derived SSTs may be just a particular feature for the year 2011 and not representative of what happened over the last few centuries.

To test the effect of seasonality and diagenetic alkenone alteration around Iceland, we compared $U^{K'}_{37}$-SST signals from all surface sediments with annual mean and seasonal SSTs (derived from the WOA09 database; Locarnini et al., 2010) (Fig. 6a; color code as in Fig. 1). $U^{K'}_{37}$-derived SSTs show a good linear correlation with annual mean SSTs, although absolute temperature values are higher at each station, with temperature differences ranging from 1 to 4 °C (Fig. 6a), generally higher than the calibration error, i.e., 1.5 °C (Müller et al., 1998) and with the highest deviations for the northernmost stations. When we compared $U^{K'}_{37}$-derived temperature values with SST from different seasons, the best fit is obtained with the summer mean SSTs (Fig. 6b). This is in agreement with peak alkenone fluxes recorded in our sediment trap during late spring and early summer. Thus, the

Table 3. Proxy-derived temperatures at St 1 in the northern part of the Iceland Basin in sedimenting particles and surface sediment and measured temperature data from satellite observations (AVHRR, NOAA) and from the climate database WOA09 (Locarnini et al., 2010).

	Temperature (°C)					
	$U_{37}^{K'}$	TEX_{86}	TEX_{86}^L	TEX_{86}^L 0–200 m	LDI	Measured
SPM July 2011, 5 m	10.8	13.4	11.1	n.d.	n.d.	
SMP July 2012, 20 m	12.4	14.4	8.8	n.d.	3.4	
Satellite July 2011						11.3
Satellite July 2012						12.9
Flux-weighted mean	7.1	8.5	14.5	11.7	−2.7	
Surface sediment	10.7	9.2	14.0	11.4	−1.3	
WOA09 annual mean 0 m						9.4
WOA09 annual mean 0–200 m						8.7

n.d.: not detected

sedimentary signal of $U_{37}^{K'}$-SST around Iceland seems in general to reflect the maximum production season of alkenones.

4.2 TEX_{86}

GDGTs in the marine environment are likely biosynthesized by Thaumarchaeota (Sinninghe Damsté et al., 2002), which are omnipresent in the global ocean, including the polar regions (e.g., Hoefs et al., 1997; DeLong et al., 1998; Schouten et al., 2000). TEX_{86}^L was developed for polar oceans in order to improve the correlation between TEX_{86} and SST (Kim et al., 2010), but a recent study has shown that TEX_{86} is still suitable as well (Ho et al., 2014). The TEX_{86}^L-SST estimates in the SPM around Iceland showed a highly variable relationship with in situ temperatures, showing temperatures up to 6 °C higher around Iceland during 2011 (Fig. 2a), while for the SPM transect, the TEX_{86}^L-SST temperatures were up to 7 °C lower compared to summer temperatures at 50 m water depth obtained from the WOA09 database (Fig. 2b). Even higher offsets, both positive and negative, up to 11 °C, were obtained with TEX_{86}-SST estimates (Fig. 2a, b). A reason for the poor correspondence of TEX_{86}-derived temperatures with in situ and satellite temperatures could be a depth habitat effect, since Thaumarchaeota can thrive deep in the marine water column (Karner et al., 2001; Herndl et al., 2005), although they tend to have their highest cell numbers at depths < 200 m (e.g., Karner et al., 2001). We also applied a specific TEX_{86} SPM calibration proposed by Schouten et al. (2013), but temperatures did still show significant offsets with in situ temperatures (data not shown).

Part of the mismatch may be due to the fact that Thaumarchaeota are smaller in cell size than the 0.7 µm pore diameter of the SPM filters (Könneke et al., 2005) and thus may not be quantitatively captured on the GFFs (Ingalls et al., 2012), possibly affecting the TEX_{86} values. However, other studies have shown comparable TEX_{86} values obtained with both 0.7 and 0.2 µm pore diameter filters (e.g., Herfort et al., 2007) or

good correspondence with depth (Schouten et al., 2012) or seasonal (Pitcher et al., 2011) profiles of isoprenoidal GDGT concentrations from 0.7 µm pore diameter filters and thaumarchaeotal rRNA gene abundances from 0.2 µm pore diameter filters. Thus, the filter size is unlikely to have affected TEX_{86} values. Another issue may be that we analyzed saponified SPM filters, combining both intact and core (nonintact) GDGT-based lipids. In the natural environment, core lipid GDGTs are derived to a substantial portion from dead cells and may thus represent a fossil signal from other areas or represent an integrated annual temperature signal. Lipp and Hinrichs (2009) showed notable differences in derived temperatures using core vs. intact polar lipid (IPL) GDGTs from marine sediments. Usually, TEX_{86}-derived temperatures are higher for IPL GDGTs than for core GDGTs, as was observed in SPM from the Arabian Sea (Schouten et al., 2012); thus, reduced TEX_{86}-derived SSTs from the SPM transect may related to core-GDGT contributions. However, this does not fully explain the dissimilarities observed in the SPM around Iceland, and thus we lack a clear explanation.

Regarding sedimenting particles, TEX_{86}^L-derived SSTs (Fig. 4, blue line and open circles) were all much higher (up to ca. 9 °C) than satellite SSTs. Reduced differences (up to ca. 5 °C higher than satellite SSTs) were obtained when temperature values were estimated using the TEX_{86}^L 0–200 m calibration (Kim et al., 2012b) (Fig. 4, red line and open circles and dashed purple line). Interestingly, differences in temperature decreased significantly when TEX_{86}-derived temperature and satellite-derived SST were compared (Fig. 4; dark blue line and filled circles), particularly during times of low GDGT fluxes (Fig. 3d). During times of high GDGT fluxes, TEX_{86}-SST were lower than satellite SST by up to 4.6 °C, which may suggest that the temperature signal is not derived just from surface waters. This is supported by TEX_{86} temperature values from SPM collected at St 1 during both cruises; TEX_{86}-derived temperatures from the surface waters are slightly higher than the satellite SSTs,
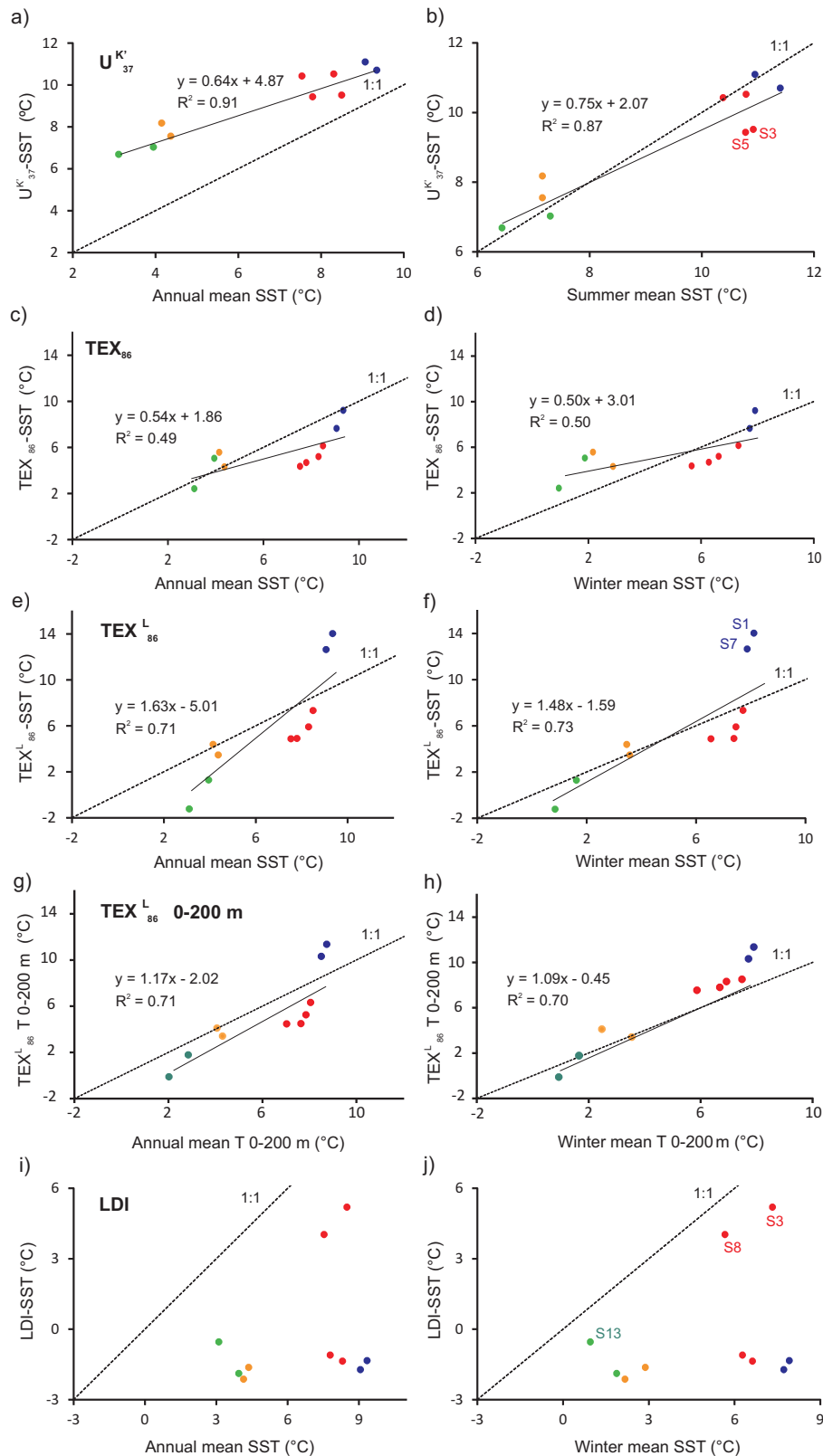
Figure 6. Crossplots of surface-sediment-proxy-derived temperatures ($U^{K'}_{37}$, TEX_{86}, TEX^{L}_{86}, TEX^{L}_{86} 0–200 m and LDI) with annual and seasonal mean temperatures (only the best seasonal correlations are shown) from the WOA09 database. Regression lines are represented as black lines, and diagonal black dashed lines show the 1 : 1 correlation. Different colors indicate different station locations, as in Fig. 1.

and significantly higher than the TEX_{86} values derived from the material collected in the same months in the sediment trap at 1850 m water depth. We observed notable differences in estimated temperatures when we used different calibrations, obtaining better results with the TEX_{86} calibration (Kim et al., 2010). Similar findings were made by Ho et al. (2014), who applied TEX_{86}^L and TEX_{86} in different polar and subpolar regions, such as the Pacific sector of the Southern Ocean and the Subarctic Front in the North Pacific. Lateral transport of GDGTs is not likely to have an effect on TEX_{86} temperatures since isoprenoid GDGTs are less susceptible to long-distance advection than alkenones (Mollenhauer et al., 2008; Shah et al., 2008; Kim et al., 2009a). Short-term degradation has also been shown to have no significant impact on the TEX_{86} (Schouten et al., 2004; Kim et al., 2009b). Terrigenous GDGTs are also unlikely to be the reason for the offset in estimated temperatures around Iceland, based on the low values of the BIT index (< 0.01) (Weijers et al., 2006, 2009) and the low correlation ($R^2 < 0.08$) between the BIT index and TEX_{86} values (cf. Schouten et al., 2013). Comparison of the flux-weighted mean TEX_{86} value with surface sediment at St 1 shows similar values, i.e., 8.5 and 9.2 °C using TEX_{86}-SST, 14.5 and 14.0 °C using TEX_{86}^L-SST, and 11.7 and 11.4 °C for TEX_{86}^L 0–200 m, suggesting no alteration of the GDGT signal during transport to the sea floor (Table 3).

As with alkenones, the sinking velocities for GDGTs can be estimated by comparing TEX_{86} values in the sediment trap with observed SST. Maximum TEX_{86}-derived temperatures were observed for sampling periods 11–17 (5 January–6 May 2012) and minimum temperatures for sampling periods 4 and 18 (5–23 September 2011 and 6–24 May 2012, respectively) (Fig. 4 and Table S2). Following the method of Fischer and Karakas (2009) and Mollenhauer et al. (2015), an offset between the production of GDGTs and their fluxes at 1850 m water depth of 4–6 months would result in estimated average sinking velocities (0–1850 m) of ca. 10–15 m d^{-1}, slower than that for the alkenones. However, it should be noted that this estimate is highly uncertain, as TEX_{86} temperatures do not show a clear seasonal trend in comparison to SST (Fig. 4).

GDGT fluxes were high during July, September and October 2011, followed by May and June 2012 (Fig. 3d), and showed similar patterns to bulk sediment flux and primary production (Fig. 3a, b). Similar GDGT flux patterns, i.e., high fluxes at times of high primary productivity, have been observed in the Arabian Sea (Wuchter et al., 2006), the Santa Barbara Basin, off the coast of southern California (Huguet et al., 2007), and the upwelling region off Cape Blanc in Mauritania (Mollenhauer et al., 2015). This was explained by a more efficient transport of thaumarchaeotal cells, and thus GDGTs, to deeper waters by the packaging activity of zooplankton thriving after a phytoplankton bloom. This could be also the case in the northern Iceland Basin, where the bulk sediment flux may act as an important mechanism for trans-

porting these lipids to the seafloor. However, the fact that highest fluxes are observed in late summer does not mean that the annual TEX_{86} signal here also represents summer temperatures, as previously suggested by Ho et al. (2014) for surface sediments from the Arctic, northern Pacific and Southern Ocean, since the flux-weighted mean TEX_{86} value from the sediment trap, and the TEX_{86} value from the underlying sediment are both similar to annual mean SST (Table 3).

TEX_{86}- and TEX_{86}^L-derived SST in the surface sediments distributed around Iceland correlate with WOA09 annual mean SSTs (Fig. 6c, e), although they do show a substantial offset, varying from 1 to 4.7 °C. A similar fit is obtained with winter mean temperatures (Fig. 6d, f), whereas the correlation with summer mean temperatures is substantially poorer (data not shown). This latter observation agrees with the idea that the highest GDGT flux during summer does not automatically result in a TEX_{86} signal, which records late summer temperatures (Fig. 3d). This is in contrast with observations by Ho et al. (2014), who showed anomalously high SST estimates in surface sediments from the Arctic, northern Pacific and Southern Ocean, and obtained the best correlation of TEX_{86}-SSTs with summer SSTs.

To test if the sedimentary TEX_{86} signal around Iceland mainly reflects subsurface temperature waters as suggested for some other regions (e.g., Huguet et al., 2007; Lopes dos Santos et al., 2010; Kim et al., 2012a, b), we compared TEX_{86}^L 0–200 m temperature estimates (Kim et al., 2012b) with the temperature of the upper 200 m of the water column based on WOA09. We obtained a better correspondence with both annual and winter mean temperatures (Fig. 6g, h), with differences ranging from 0.5 to 3.5 °C. This suggests that TEX_{86}-derived signals in the surface sediments around Iceland may reflect subsurface (i.e., 0–200 m) temperatures.

4.3 LDI

Long-chain alkyl diols, either the 1,13- and 1,15-diols involved in the LDI or the 1,14-diols produced by *Proboscia* diatoms (Sinninghe Damsté et al., 2003) and *Apedinella radians* (Rampen et al., 2011), were below the detection limit in SPM sampled around Iceland in summer 2011. In the SPM sampled during the 2012 transect, small amounts of long-chain 1,15-, 1,14- and 1,13-diols were detected. This suggests that July is not a period of high productivity for long-chain diol producers around Iceland. However, long-chain 1,13- and 1,15-diol mass fluxes were relatively high during July, September and October 2011 and from May to July 2012 (Fig. 3e), suggesting that diol producers were present, although not at the time, depths or exact locations as where the SPM was sampled. This suggests a patchy distribution of diol producers. Indeed, it has been observed that diatom distribution and composition around Iceland is highly variable and strongly influenced by different environmental variables

and particularly by summer sea surface temperature (Jiang et al., 2001).

Interestingly, the fluxes of 1,13- and 1,15-diols were always much lower than C_{28} and C_{30} saturated and monounsaturated 1,14-diol fluxes, as well as 3 orders of magnitude lower than those of alkenones and GDGTs. This indicates that 1,13- and 1,15-diols and their producers are not abundant in this environment. The presence of C_{28} and C_{30} saturated and monounsaturated 1,14-diol fluxes suggests that *Proboscia* diatoms have bloomed in late summer and autumn and late spring and summer. This is further supported by the identification of C_{27} and C_{29} mid-chain hydroxyl methyl alkanoates in the sedimenting particles (data not shown), which are also biomarker lipids from *Proboscia* diatoms (Sinninghe Damsté et al., 2003). Interestingly, trace amounts of both C_{28} and C_{30} 1,13-diols have been identified in *Proboscia* species (Rampen et al., 2007), and the relatively high abundance of saturated and monosaturated 1,14-diols, combined with a similar flux pattern as that of the 1,13 and 1,15-diols, suggests that *Proboscia* may also be a source for the 1,13- and 1,15-diols in this area.

Where LDI values could be calculated for the SPM, temperatures were substantially lower than satellite SSTs (Fig. 2b), exceeding the calibration error of 2 °C (Rampen et al., 2012). For the sediment trap, LDI values were not always calculated due to the nonquantifiable amount of C_{30} 1,15-diol. For cases where it was possible, the temperature values were, like the SPM, much lower than satellite temperatures (Fig. 4, brown line and open squares; Table 3). The eukaryotic phytoplankton generally responsible for the production of 1,13- and 1,15-diols are likely eustigmatophyte algae, autotrophs living in the upper photic zone (Volkman et al., 1992; Rampen et al., 2012), and on a global scale, the LDI correlates best with late summer and early autumn SST (cf. Rampen et al., 2012). Thus, a contribution from colder deep water is unlikely to explain the low temperatures observed with the LDI. A similar observation is made for the LDI-derived SSTs in the surface sediments around Iceland which are always lower than annual mean SST, even when compared with the coldest season, i.e., winter mean SST (Fig. 6i, j). Furthermore, there is no correlation of LDI values with SST. Also in the surface sediments, relatively low abundances of 1,13- and 1,15-diols compared to 1,14-diols were observed. The mismatch of LDI values with temperature as well as the low abundances of long-chain 1,13- and 1,15-alkyl diols reinforce the hypothesis that *Proboscia* diatoms seem to be at least a partial source of 1,13- and 1,15-diols in the Iceland region. This suggests that the LDI may not be applicable in this region. Therefore, we advise that, if 1,14-diols dominate the distributions of long-chain alkyl diols, the LDI should be applied with great caution.

5 Conclusions

The application of three independent organic temperature proxies at high latitudes was studied in the region around Iceland. $U_{37}^{K'}$-derived SSTs in SPM and sedimenting particles are generally lower than annual mean SST. In contrast, $U_{37}^{K'}$-derived SSTs in the surface sediments around Iceland correlate well with summer mean SST, which seems in agreement with the observation of elevated alkenone fluxes during late spring and early summer. The mismatch between the flux-weighted mean $U_{37}^{K'}$-derived SST and the $U_{37}^{K'}$-derived SST from the underlying surface sediment may be due to diagenetic alkenone alteration during the sedimentation process or because an unusual year was sampled with the sediment trap.

High fluxes of the isoprenoidal GDGTs used in the TEX_{86} proxy were observed during warmer months with high productivity and mass fluxes, which may be explained by a preferential transport of GDGTs to deeper waters by the packaging activity of zooplankton thriving after a phytoplankton bloom. However, the flux-weighted mean TEX_{86} value corresponds well with annual mean SST in surface sediments, TEX_{86}-derived temperatures showed a good correlation with both annual and winter mean 0–200 m temperatures, suggesting that the TEX_{86} signal is primarily derived from these subsurface waters.

The LDI around Iceland did not show any relationship with SST. The similarity in trends between all long-chain alkyl diols and the dominant abundances of 1,14-diols over 1,13- and 1,15-diols may suggest that the *Proboscia* diatom is an important source of 1,13- and 1,15-diols in the Iceland region, limiting the LDI application in this area. Therefore, we advise caution in interpreting LDI values in areas where 1,14-diols strongly dominate the long-chain alkyl diol distributions.

Data availability

Data from this publication are archived in the data center "Pangaea" (www.Pangaea.de).

The Supplement related to this article is available online at doi:10.5194/bg-12-6573-2015-supplement.

Author contributions. J. S. Sinninghe Damsté and S. W. Rampen designed the research. S. W. Rampen, M. Baas and H. de Haas performed the sampling. M. Rodrigo-Gámiz performed the experimental laboratory work. M. Rodrigo-Gámiz, S. W. Rampen, S. Schouten and J. S. Sinninghe Damsté prepared the manuscript.

References

Baas, M. and Koning, E.: Cruise report R.V. Pelagia 64PE357, Diols-Trap Recovery, Reykjavik – Reykjavik, available at: http://melia.nioz.nl/public/dmg/rpt/crs/64pe357.pdf, last access: 23–29 July 2012.

Baumann, K.-H., Andruleit, H. A., and Samtleben, C.: Coccolithophores in the Nordic Seas: comparison of living communities with surface sediment assemblages, Deep-Sea Res. Pt. II, 47, 1743–1772, 2000.

Behrenfeld, M. J. and Falkowski, P. G.: Photosynthetic rates derived from satellite-based chlorophyll concentration, Limnol. Oceanogr., 42, 1–20, 1997.

Brassell, S. C., Eglinton, G., Marlowe, I. T., Pflaumann, U., and Sarnthein, M.: Molecular stratigraphy: A new tool for climatic assessment, Nature, 320, 129–133, 1986.

Conte, M. H., Sicre, M. -A., Rühlemann, C., Weber, J. C., Schulte, S., Schulz-Bull, D., and Blanz, T.: Global temperature calibration of the alkenone unsaturation index ($U_{37}^{K'}$) in surface waters and comparison with surface sediments, Geochem. Geophys. Geosyst., 7, Q02005, doi:10.1029/2005GC001054, 2006.

de Haas, H.: Cruise report R.V. Pelagia 64PE341, Long Chain Diols (LCD), Texel – Reykjavik, available at: http://melia.nioz.nl/public/dmg/rpt/crs/64pe341.pdf, last access: 7–22 July 2011.

De Leeuw, J. W., Rijpstra, W. I. C., Schenck, P. A., and Volkman, J.: Free, esterified and residual sterols in Black Sea Unit I sediments, Geochim. Cosmochim. Ac., 47, 455–465, 1983.

DeLong, E. F., King, L. L., Massana, R., Cittone, H., Murray, A., Schleper, C., and Wakeham, S. G.: Dibiphytanyl ether lipids in nonthermophilic crenarchaeotes, Appl. Environ. Microbiol., 64, 113–1138, 1998.

Fischer, G. and Karakas, G.: Sinking rates and ballast composition of particles in the Atlantic Ocean: implications for the organic carbon fluxes to the deep ocean, Biogeosciences, 6, 85–102, doi:10.5194/bg-6-85-2009, 2009.

Gelin, F., Boogers, I., Noordeloos, A. A. M., Sinninghe Damsté, J. S., Riegman, R., and de Leeuw, J. W.: Resistant biomacromolecules in marine microalgae of the classes Eustigmatophyceae and Chlorophyceae: Geochemical implications, Org. Geochem., 26, 659–675, 1997.

Gong, C. and Hollander, D. J.: Evidence for differential degradation of alkenones under contrasting bottom water oxygen conditions: Implications for paleotemperature reconstruction, Geochim. Cosmochim. Ac., 63, 405–411, 1999.

Hanna, E., Jonsson, T., Ólafsson, J., and Vladimarsson, H.: Icelandic coastal sea surface temperature records constructed: putting the pulse on air–sea climate interactions in the Northern North Altantic, Part I: Comparison with HadISST1 open-ocean surface temperatures and preliminary analysis of long-term patterns and anomalies of SSTs around Iceland, J. Clim., 19, 5652–5666, 2006.

Harada, N., Sato, M., Shiraishi, A., and Honda, M. C.: Characteristics of alkenone distributions in suspended and sinking particles in the northwestern North Pacific. Geochim. Cosmochim. Ac., 70, 2045–2062, 2006.

Herfort, L., Schouten, S., Abbas, B., Veldhuis, M. J. W., Coolen, M. J. L., Wuchter, C., Boon, J. P., Herndl, G. J., and Sinninghe Damsté, J. S.: Variations in spatial and temporal distribution of Archaea in the North Sea in relation to environmental variables, FEMS Microbiol. Ecol., 62, 242–257, 2007.

Herndl, G. J., Reinthaler, T., Teira, E., van Aken, H., Veth, C., Pernthaler, A., and Pernthaler, J.: Contribution of Archaea to total prokaryotic production in the deep Atlantic Ocean, Appl. Environ. Microbiol., 71, 2303–2309, 2005.

Ho, S. L., Mollenhauer, G., Fietz, S., Martínez-Garcia, A., Lamy, F., Rueda, G., Schipper, K., Méheust, M., Rosell-Melé, A., Stein, R., and Tiedemann, R.: Appraisal of TEX_{86} and TEX_{86}^L thermometries in subpolar and polar regions, Geochim. Cosmochim. Ac., 131, 213–226, 2014.

Hoefs, M. J. L., Schouten, S., King, L. L., Wakeham, S. G., de Leeuw, J. W., and Sinninghe Damsté, J. S.: Ether lipids of planktonic archaea in the marine water column, Appl. Environ. Microbiol., 63, 3090–3095, 1997.

Hoefs, M. J. L., Versteegh, G. J. M., Rijpstra, W. I. C., de Leeuw, J. W., and Sinninghe Damsté, J. S.: Postdepositional oxic degradation of alkenones: Implications for the measurement of palaeo sea surface temperatures, Paleoceanography, 13, 42–49, 1998.

Hopkins, T. S.: The GIN Sea – a synthesis of its physical oceanography and literature review 1972–1985, Earth Sci. Rev., 30, 175–318, 1991.

Hopmans, E. C., Weijers, J. W. H., Schefuß, E., Herfort, L., Sinninghe Damsté, J. S., and Schouten, S.: A novel proxy for terrestrial organic matter in sediments based on branched and isoprenoid tetraether lipids, Earth Planet. Sci. Lett., 224, 107–116, 2004.

Huguet, C., Hopmans, E. C., Febo-Ayala, W., Thompson, D. H., Sinninghe Damsté, J. S., and Schouten, S.: An improved method to determine the absolute abundance of glycerol dibiphytanyl glycerol tetraether lipids, Org. Geochem., 37, 1036–1041, 2006.

Huguet, C., Schimmelmann, A., Thunell, R., Lourens, L. J., Sinninghe Damsté, J. S., and Schouten, S.: A study of the TEX_{86} paleothermometer in the water column and sediments of the Santa Barbara Basin, California, Paleoceanography, 22, PA3203, doi:10.1029/2006PA001310, 2007.

Ingalls, A. E., Huguet, C., and Truxal, L. T.: Distribution of intact and core membrane lipids of archaeal glycerol dialkyl glycerol tetraethers among size-fractionated particulate organic matter in Hood Canal, Puget Sound, Appl. Environ. Microbiol., 78, 1480–1490, 2012.

Jiang, H., Seidenkrantz, M. S., Knudsen, K. L., and Eiríksson, J.: Diatom surface sediment assemblages around Iceland and their relationships to oceanic environmental variables, Mar. Micropaleontol., 41, 73–96, 2001.

Karner, M. B., DeLong, E. F., and Karl, D. M.: Archaeal dominance in the mesopelagic zone of the Pacific Ocean, Nature, 409, 507–510, 2001.

Kim, J.-H., Schouten, S., Hopmans, E. C., Donner, B., and Sinninghe Damsté, J. S.: Global sediment core-top calibration of the TEX86 paleothermometer in the ocean, Geochim. Cosmochim. Ac., 72, 1154–1173, 2008.

Kim, J.-H., Crosta, X., Michel, E., Schouten, S., Duprat, J., and Sinninghe Damsté, J. S.: Impact of lateral transport on organic proxies in the Southern Ocean, Quat. Res., 71, 246–250, 2009a.

Kim, J.-H., Huguet, C., Zonneveld, K. A. F., Versteegh, G. J. M., Roeder, W., Sinninghe Damsté, J. S., and Schouten, S.: An experimental field study to test the stability of lipids used for TEX$_{86}$ and U$_{37}^{K'}$ palaeothermometry, Geochim. Cosmochim. Ac., 73, 2888–2898, 2009b.

Kim, J.-H., van der Meer, J., Schouten, S., Helmke, P., Willmott, V., Sangiorgi, F., Koç, N., Hopmans, E. C., and Sinninghe Damsté, J. S.: New indices and calibrations derived from the distribution of crenarchaeal isoprenoid tetraether lipids: Implications for past sea surface temperature reconstructions, Geochim. Cosmochim. Ac., 74, 4639–4654, 2010.

Kim, J.-H., Romero, O. E., Lohmann, G., Donner, B., Laepple, T., Haam, E., and Sinninghe Damsté, J. S.: Pronounced subsurface cooling of North Atlantic waters off Northwest Africa during Dansgaard-Oeschger interstadials, Earth Planet. Sci. Lett., 339, 95–102, 2012a.

Kim, J.-H., Crosta, X., Willmott, V., Renssen, H., Bonnin, J., Helmke, P., Schouten, S., and Sinninghe Damsté, J. S.: Holocene subsurface temperature variability in the eastern Antarctic continental margin, Geophys. Res. Lett., 39, L06705, doi:10.1029/2012GL051157, 2012b.

Könneke, M., Bernhard, A. E., de la Torre, J. R., Walker, C. B., Waterbury, J. B., and Stahl, D. A.: Isolation of an autotrophic ammonia-oxidizing marine archaeon, Nature, 437, 543–546, 2005.

Lee, K. E., Khim, B. K., Otosaka, S., and Noriki, S.: Sediment trap record of alkenones from the East Sea (Japan Sea), Org. Geochem., 42, 255–261, 2011.

Lipp, J. S. and Hinrichs, K.-U.: Structural diversity and fate of intact polar lipids in marine sediments, Geochim. Cosmochim. Acta, 73, 6816–6833, 2009.

Locarnini, R. A., Mishonov A. V., Antonov, J. I., Boyer, T. P., Garcia, H. E., Baranova, O. K., Zweng, M. M., and Johnson, D. R.: World Ocean Atlas 2009: Volume 1: Temperature, in: NOAA Atlas NESDIS 68, edited by: Levitus, S., US Government Printing Office, Washington, DC, 184 pp., 2010.

Lopes dos Santos, R. A., Spooner, M. I., Barrows, T. T., De Deckker, P., Sinninghe Damsté, J. S., and Schouten, S.: Comparison of organic (U$_{37}^{K'}$, TEX$_{86}^{H}$, LDI) and faunal proxies (foraminiferal assemblages) for reconstruction of late Quaternary sea-surface temperature variability from offshore southeastern Australia, Paleoceanography, 28, 377–387, 2013.

Malmberg, S.-A. and Jónsson, S.: Timing of deep convection in the Greenland and Iceland Seas, ICES J. Mar. Sci., 54, 300–309, 1997.

Marlowe, I. T., Green, J. C., Neal, A. C., Brassell, S. C., Eglinton, G., and Course, P. A.: Long-chain (n-C$_{37}$–C$_{39}$) alkenones in the Prymnesiophyceae. Distribution of alkenones and other lipids and their taxonomic significance, Brit. Phycol. J., 19, 203–216, 1984.

Méjanelle, L., Sanchez-Gargallo, A., Bentaleb, I., and Grimalt, J. O.: Long chain n-alkyl diols, hydroxy ketones and sterols in a marine eustigmatophyte, Nannochloropsis gaditana, and in Brachionus plicatilis feeding on the algae, Org. Geochem., 34, 527–538, 2003.

Mollenhauer, G., Eglinton, T. I., Hopmans, E. C., and Sinninghe Damsté, J. S.: A radiocarbon-based assessment of the preservation characteristics of crenarchaeol and alkenones from continental margin sediments, Org. Geochem., 39, 1039–1045, 2008.

Mollenhauer, G., Basse, A., Kim, J.-H., Sinninghe Damsté, J. S., and Fischer, G.: A four-year record of U$_{37}^{K'}$- and TEX$_{86}$-derived sea surface temperature estimates from sinking particles in the filamentous upwelling region off Cape Blanc, Mauritania, Deep-Sea Res. Pt. I, 97, 67–79, 2015.

Müller, P. J. and Fischer, G.: A 4-year sediment trap record of alkenones from the filamentous upwelling region off Cape Blanc, NW Africa and a comparison with distributions in underlying sediments, Deep-Sea Res. Pt. I, 48, 1877–1903, 2001.

Müller, P. J., Kirst, G., Ruhland, G., von Storch, I., and Rossell-Melé, A.: Calibration of alkenone paleotemperature index U$_{37}^{K'}$ based on core tops from the eastern South Atlantic and the global ocean (60° N–60° S), Geochim. Cosmochim. Ac., 62, 1757–1771, 1998.

Ólafsson, J.: Connections between oceanic conditions off N-Iceland, Lake Mývatn temperature, regional wind direction variability and the North Atlantic Oscillation, Rit Fiskideildar, 16, 41–57, 1999.

Pitcher, A., Wuchter, C., Siedenberg, K., Schouten, S., and Sinninghe Damsté, J. S.: Crenarchaeol tracks winter blooms of ammonia-oxidizing Thaumarchaeota in the coastal North Sea, Limnol. Oceanogr., 56, 2308–2318, 2011.

Popp, B. N., Prahl, F. G., Wallsgrove, R. J., and Tanimoto, J.: Seasonal patterns of alkenone production in the subtropical oligotrophic North Pacific, Paleoceanogeaphy, 21, PA1004, doi:10.1029/2005PA001165, 2006.

Prahl, F. G. and Wakeham, S.G.: Calibration of unsaturation patterns in long-chain ketone compositions for paleotemperature assessment, Nature, 330, 367–369, 1987.

Prahl, F. G., Muehlhausen, L. A., and Zahnle, D. B.: Further evaluation of long-chain alkenones as indicators of paleoceanographic conditions, Geochim. Cosmochim. Ac., 52, 2303–2310, 1988.

Prahl, F. G., Dymond, J., and Sparrow, M. A.: Annual biomarker record for export production in the central Arabian Sea. Deep-Sea Res. Pt. II, 47, 1581–1604, 2000.

Prahl, F. G., Pilskaln, C. H., and Sparrow, M. A.: Seasonal record for alkenones in sedimentary particles from the Gulf of Maine, Deep-Sea Res. Pt. I, 48, 515–528, 2001.

Prahl, F. G., Sparrow, M. A., and Wolfe, G. V.: Physiological impacts on alkenone paleothermometry, Paleoceanography, 18, 1025, doi:10.1029/2002PA000803, 2003.

Rampen, S. W., Schouten, S., Wakeham, S. G., and Sinninghe Damsté, J. S.: Seasonal and spatial variation in the sources and fluxes of long chain diols and mid-chain hydroxy methyl alkanoates in the Arabian Sea, Org. Geochem., 38, 165–179, 2007.

Rampen, S. W., Schouten, S., and Sinninghe Damsté, J. S.: Occurrence of long chain 1,14 diols in Apedinella radians, Org. Geochem., 42, 572–574, 2011.

Rampen, S. W., Willmott, V., Kim, J. -H., Uliana, E., Mollenhauer, G., Schefuß, E., Sinninghe Damsté, J. S., and Schouten, S.: Long chain 1,13- and 1,15-diols as a potential proxy for palaeotemperature reconstruction, Geochim. Cosmochim. Ac., 84, 204–216, 2012.

Rodrigo-Gámiz, M., Martínez-Ruiz, F., Rampen, S. W., Schouten, S., and Sinninghe Damsté, J. S.: Sea surface temperature variations in the western Mediterranean Sea over the last 20 kyr: A dual-organic proxy ($U_{37}^{K'}$ and LDI) approach, Paleoceanography, 29, 87–98, 2014.

Rontani, J.-F., Volkman, J. K., Prahl, F. G., and Wakeham, S.G.: Biotic and abiotic degradation of alkenones and implications for $U_{37}^{K'}$ paleoproxy applications: A review, Org. Geochem., 59, 95–113, 2013.

Rosell-Melé, A.: Interhemispheric appraisal of the value of alkenone indices as temperature and salinity proxies in high-latitude locations, Paleoceanography, 13, 694–703, 1998.

Rosell-Melé, A. and Comes, P.: Evidence for a warm Last Glacial Maximum in the Nordic seas or an example of shortcomings in $U_{37}^{K'}$ and U_{37}^{K} to estimate low sea surface temperature?, Paleoceanography, 14, 770–776, 1999.

Rosell-Melé, A. and Prahl, F. G.: Seasonality of $U_{37}^{K'}$ temperature estimates as inferred from sediment trap data, Quat. Sci. Rev., 72, 128–136, 2013.

Rosell-Melé, A., Carter, J., and Eglinton, G.: Distributions of long-chain alkenones and alkyl alkenoates in marine surface sediments from the North East Atlantic, Org. Geochem., 22, 501–509, 1994.

Rosell-Melé, A., Comes, P., Müller, P. J., and Ziveri, P.: Alkenone fluxes and anomalous $U_{37}^{K'}$ values during 1989–1990 in the Northeast Atlantic (48° N 21° W), Mar. Chem., 71, 251–264, 2000.

Schouten, S., Hopmans, E. C., Pancost, R. D., and Sinninghe Damsté, J. S.: Widespread occurrence of structurally diverse tetraether membrane lipids: Evidence for the ubiquitous presence of low-temperature relatives of hyperthermophiles, PNAS 97, 14421–14426, 2000.

Schouten, S., Hopmans, E. C., Schefuß, E., and Sinninghe Damsté, J. S.: Distributional variations in marine crenarchaeotal membrane lipids: A new tool for reconstructing ancient sea water temperatures?, Earth. Planet. Sci. Lett., 204, 265–274, 2002.

Schouten, S., Hopmans, E. C., and Sinninghe Damsté, J. S.: The effect of maturity and depositional redox conditions on archaeal tetraether lipid palaeothermometry, Org. Geochem., 35, 567–571, 2004.

Schouten, S., Huguet, C., Hopmans, E. C., Kienhuis, M. V. M., and Sinninghe Damsté, J. S.: Analytical methodology for TEX$_{86}$ paleothermometry by high-performance liquid chromatography/atmospheric pressure chemical ionization-mass spectrometry, Anal. Chem., 79, 2940–2944, 2007.

Schouten, S., Pitcher, A., Hopmans, E. C., Villanueva, L., van Bleijswijk J., and Sinninghe Damsté, J. S.: Intact polar and core glycerol dibiphytanyl glycerol tetraether lipids in the Arabian Sea oxygen minimum zone: I. Selective preservation and degradation in the water column and consequences for the TEX$_{86}$, Geochim. Cosmochim. Ac., 98, 228–243, 2012.

Schouten, S., Hopmans, E. C., and Sinninghe Damsté, J. S.: The organic geochemistry of glycerol dialkyl glycerol tetraether lipids: A review, Org. Geochem., 54, 19–61, 2013.

Seki, O., Nakatsuka, T., Kawamura, K., Saitoh, S.-I., and Wakatsuchi, M.: Time-series sediment trap record of alkenones from the western Sea of Okhotsk. Mar. Chem., 104, 253–265, 2007.

Sell, D. W. and Evans, M. S.: A statistical analysis of subsampling and an evaluation of the Folsom plankton splitter, Hydrobiologia, 94, 223–230, 1982.

Shah, S. R., Mollenhauer, G., Ohkouchi, N., Eglinton, T. I., and Pearson, A.: Origins of archaeal tetraether lipids in sediments: insights from radiocarbon analysis, Geochim. Cosmochim. Ac., 72, 4577–4594, 2008.

Sicre, M.-A., Bard, E., Ezat, U., and Rostek, F.: Alkenone distributions in the North Atlantic and Nordic sea surface waters, Geochem., Geophys., Geosyst., 3, 1–13, 2002.

Sicre, M.-A., Labeyrie, L., Ezat, U., Duprat, J., Turon, J. -L., Schmidt, S., Michel, E., and Mazaud, A.: Mid-Latitude southern ocean response to northern hemisphere Heinrich events, Earth Planet. Sci. Lett., 240, 724–731, 2005.

Sicre, M.-A., Labeyrie, L., Ezat, U., Duprat, J., Turon, J.-L., Schmidt, S., Michel, E., and Mazaud, A.: Erratum to: Mid-Latitude southern ocean response to northern hemisphere Heinrich events, Earth Planet. Sci. Lett., 243, 303–304, 2006.

Sigtryggsson, H.: An outline of sea ice conditions in the vicinity of Iceland, Jökull, 22, 1–11, 1972.

Sikes, E. L. and Volkman, J. K.: Calibration of alkenone unsaturation ratios ($U_{37}^{K'}$) for paleotemperature estimation in cold polar waters, Geochim. Cosmochim. Ac., 57, 1883–1889, 1993.

Sikes, E. L., Volkman, J. K., Robertson, L. G., and Pichon, J. -J.: Alkenones and alkenes in surface waters and sediments of the Southern Ocean: implications for paleotemperature estimation in polar regions, Geochim. Cosmochim. Ac., 61, 1495–1505, 1997.

Sikes, E. L., O'Leary, T., Nodder, S. D., and Volkman, J. K.: Alkenone temperature records and biomarker flux at the subtropical front on the Chatham rise, SW Pacific Ocean, Deep-Sea Res. Pt. I, 52, 721–748, 2005.

Sinninghe Damsté, J. S., Hopmans, E. C., Schouten, S., van Duin, A. C. T., and Geenevasen, J. A. J.: Crenarchaeol: the characteristic core glycerol dibiphytanyl glycerol tetraether membrane lipid of cosmopolitan pelagic crenarchaeota, J. Lipid Res., 43, 1641–1651, 2002.

Sinninghe Damsté, J. S., Rampen, S. W., Rijpstra, W. I. C., Abbas, B., Muyzer, G., and Schouten, S.: A diatomaceous origin for long-chain diols and mid-chain hydroxy methyl alkanoates widely occurring in Quaternary marine sediments: Indicators for high nutrient conditions, Geochim. Cosmochim. Ac., 67, 1339–1348, 2003.

Smith, M., De Deckker, P., Rogers, J., Brocks, J., Hope, J., Schmidt, S., Lopes dos Santos, R., and Schouten, S.: Comparison of $U_{37}^{K'}$, TEX$_{86}^{H}$ and LDI temperature proxies for reconstruction of southeast Australian ocean temperatures, Org. Geochem., 64, 94–104, 2013.

Ternois, Y., Sicre, M.-A., Boireau, A., Conte, M. H., and Eglinton, G.: Evaluation of long-chain alkenones as paleo-temperature indicators in the Mediterranean Sea. Deep-Sea Res. Pt. I, 44, 271–286, 1997.

Ternois, Y., Sicre, M.-A., Boireau, A., Beaufort, L., Miquel, J.-C., and Jeandel, C.: Hydrocarbons, sterols and alkenones in sinking particles in the Indian sector of the Southern Ocean, Org. Geochem., 28, 489–501, 1998.

Thordardottir, Th.: Timing and duration of spring blooming south and southwest of Iceland, in: The Role of Freshwater Outflow in Coastal Marine Ecosystems, NATO ASI Series, vol. G7, edited by: Skreslet, S., Springer, Berlin, 345–360, 1986.

Versteegh, G. J. M., Bosch, H. J., and de Leeuw, J. W.: Potential palaeoenvironmental information of C_{24} to C_{36} mid-chain diols, keto-ols and mid-chain hydroxy fatty acids; a critical review, Org. Geochem., 27, 1–13, 1997.

Versteegh, G. J. M., Jansen, J. H. F., de Leeuw, J. W., and Schneider, R. R.: Mid-chain diols and keto-ols in SE Atlantic sediments: a new tool for tracing past sea surface water masses?, Geochim. Cosmochim. Ac., 64, 1879–1892, 2000.

Volkman, J. K., Eglinton, G., Corner, E. D. S., and Forsberg, T. E. V.: Long-chain alkenes and alkenones in the marine coccolithophorid *Emiliania huxleyi*, Phytochemistry, 19, 2619–2622, 1980.

Volkman, J. K., Barrett, S. M., Dunstan, G. A., and Jeffrey, S. W.: C_{30}-C_{32} alkyl diols and unsaturated alcohols in microalgae of the class Eustigmatophyceae, Org. Geochem., 18, 131–138, 1992.

Volkman, J. K., Barrett, S. M., Blackburn, S. I., and Sikes, E. L.: Alkenones in *Gephyrocapsa oceanica*: implications for studies of paleoclimate, Geochim. Cosmochim. Ac., 59, 513–520, 1995.

Volkman, J. K., Barrett, S. M., and Blackburn, S. I.: Eustigmatophyte microalgae are potential sources of C_{29} sterols, C_{22}–C_{28} *n*-alcohols and C_{28}–C_{32} *n*-alkyl diols in freshwater environments, Org. Geochem., 30, 307–318, 1999.

Weijers, J. W. H., Schouten, S., Spaargaren, O. C., and Sinninghe Damsté, J. S.: Occurrence and distribution of tetraether membrane lipids in soils: implications for the use of the TEX_{86} proxy and the BIT index, Org. Geochem., 37, 1680–1693, 2006.

Weijers, J. W. H., Schouten, S., Schefuß, E., Schneider, R. R., and Sinninghe Damsté, J. S.: Disentangling marine, soil and plant organic carbon contributions to continental margin sediments: a multiproxy approach in a 20 000 year sediment record from the Congo deep-sea fan, Geochim. Cosmochim. Ac., 73, 119–132, 2009.

Wuchter, C., Abbas, B., Coolen, M. J. L., Herfort, L., van Bleijswijk, J., Timmers, P., Strous, M., Teira, E., Herndl, G. J., Middelburg, J. J., Schouten, S., and Sinninghe Damsté, J. S.: Archaeal nitrification in the ocean, PNAS, 103, 12317–12322, 2006.

Yamamoto, M., Shimamoto, A., Fukuhara, T., Naraoka, H., Tanaka, Y., and Nishimura, A.: Seasonal and depth variations in molecular and isotopic alkenone composition of sinking particles from the western North Pacific, Deep-Sea Res. Pt. I, 54, 1571–1592, 2007.

Zhai, L., Gudmundsson, K., Miller, P., Peng, W., Gujfinnsson, H., Debes, H., Hátún, H., White III, G. N., Hernández Walls, R., Sathyendranath, S., and Platt, T.: Phytoplankton phenology and production around Iceland and Faroes, Cont. Shelf Res., 37, 15–25, 2012.